Image Cover Sheet

CLASSIFICATION	SYSTEM NUMBER
UNCLASSIFIED	513877

TITLE

A Mathematical Model of Cerebral Perfusion Subjected to Gz Acceleration

System Number:

Patron Number:

Requester:

Notes:

DSIS Use only:

Deliver to:

ORIGINAL RESEARCH

A Mathematical Model of Cerebral Perfusion Subjected to Gz Acceleration

SRDJAN CIROVIC, M.Sc., COLIN WALSH, PH.D., AND WILLIAM D. FRASER, M.Sc.

CIROVIC S, WALSH C, FRASER WD. *A mathematical model of cerebral perfusion subjected to Gz acceleration.* **Aviat Space Environ Med 2000; 71:514–21.**

Background: When the human body is exposed to a high gravitational load, the blood supply to the brain is reduced and loss of consciousness may occur. Our goal is to identify the principal mechanical causes of reduced blood supply to the brain during high +Gz. ***Methods:*** We have developed a mathematical model to investigate the influence of Gz on the cerebral circulation. Blood flow is modeled using a one-dimensional flow approximation, in which the cross-sectional area of elastic vessels is determined as a non-linear function of the transmural (blood minus external) pressure. The intracranial vessels are subjected to cerebrospinal fluid pressure (PCSF) which is determined from the condition that the cranial volume is conserved. ***Results:*** For a constant pressure difference of 100 mm Hg applied to the arterial and venous ends of the model, blood flow is diminished for +Gz. At approximately +5 Gz the blood flow predicted by the model is insufficient to maintain normal functioning of the brain. PCSF is approximately equal to the blood pressure in the large intracranial veins for all values of Gz. Extracranial arteries and the intracranial vessels do not collapse, even when Gz is substantially higher than normal. However, the extracranial veins are collapsed even for moderate +Gz. ***Conclusions:*** Even if cardiac output is maintained at normal levels, cerebral perfusion will fall because of the increasing resistance of the cerebral flow circuit. This increase is largely due to the collapse of the extracranial veins, which begins at moderate Gz and becomes dominant at a Gz of approximately 4.5.

Keywords: vascular resistance, venous resistance, transmural pressure, tube law, perfusion pressure, cerebrospinal fluid, cerebrospinal fluid pressure.

EXPOSURE TO +Gz acceleration can cause inadequate perfusion of the retina and brain leading to loss of vision and/or loss of consciousness (GLOC) (12). When Gz is greater than the normal gravitational acceleration of the Earth (+1 Gz), the weight of the blood is increased. Since the drop in the hydrostatic (gravitational) pressure with elevation is proportional to the weight of the fluid, the blood pressure at the level of the head can be expected to be zero at approximately +4.5 Gz. However, in a closed system with no net change in potential energy, such as the circulatory system, an increased hydrostatic gradient is not sufficient to explain the decrease in cerebral blood flow. If blood vessels were rigid the cerebral perfusion would not be affected by the Gz force, since the hydrostatic gradients on the arterial and venous side are equal and of the opposite sign, and the vascular resistance is independent of Gz stress. Blood flow should be independent of Gz stress and determined by the perfusion (left ventricular minus right atrial) pressure only. However, blood vessels have elastic walls and their cross-sectional area is a function of the transmural (internal minus external) pressure. In particular, thin-walled compliant vessels, such as veins, have a tendency to collapse when subjected to negative transmural pressure. If the blood pressure drop due to the hydrostatic effects is large enough, the transmural pressure will become negative causing blood vessels to collapse, decreasing the cross-sectional area of the vessel and, consequently, increasing the viscous resistance. Therefore, when vessels are compliant, the vascular resistance should be a function of the gravitational stress. Thus, blood flow would be determined by the perfusion pressure, the transmural pressure, and the elastic properties of blood vessels, at each point in the vascular network.

While it is obvious that the gravitational force directly affects the blood pressure, it is important to acknowledge that it also exerts an influence on the external pressure acting on blood vessels. Two groups of vessels can be distinguished, according to the external pressure to which they are subjected. The extracranial vessels, such as external carotid arteries and jugular veins, are subjected to the pressure of the surrounding tissue, which can be regarded as zero (atmospheric) and independent of the Gz force. On the other hand, vessels contained in the cranial cavity, are subjected to cerebrospinal fluid pressure (PCSF). Moreover, cranial blood flow and cerebrospinal fluid (CSF) dynamics are tightly connected (6,13). It is routinely assumed that the total cranial volume does not change, since the cranium is enclosed by the skull which is effectively rigid and sealed (21). Also, all three intracranial components (brain, blood, CSF) are largely comprised of water and are, therefore, essentially incompressible (17). Thus, any change of the cranial blood volume must be accompanied by an

From the Defence and Civil Institute of Environmental Medicine, North York, Ont. (W. D. Fraser), Institute for Aerospace Studies, University of Toronto, Downsview, Ont. (S. Cirovic); and Mechanical Engineering Dept., Ryerson Polytechnic University, Toronto, Ont., Canada (C. Walsh).

This manuscript was received for review in July 1998. It was revised in July 1999. It was accepted for publication in August 1999

Address reprint requests to: Srjan Cirovic, DCIEM, 1133 Sheppard Ave. West, P.O Box 2000, North York, Ont, Canada M3M 3B9; cirovics@mie.utoronto.ca.

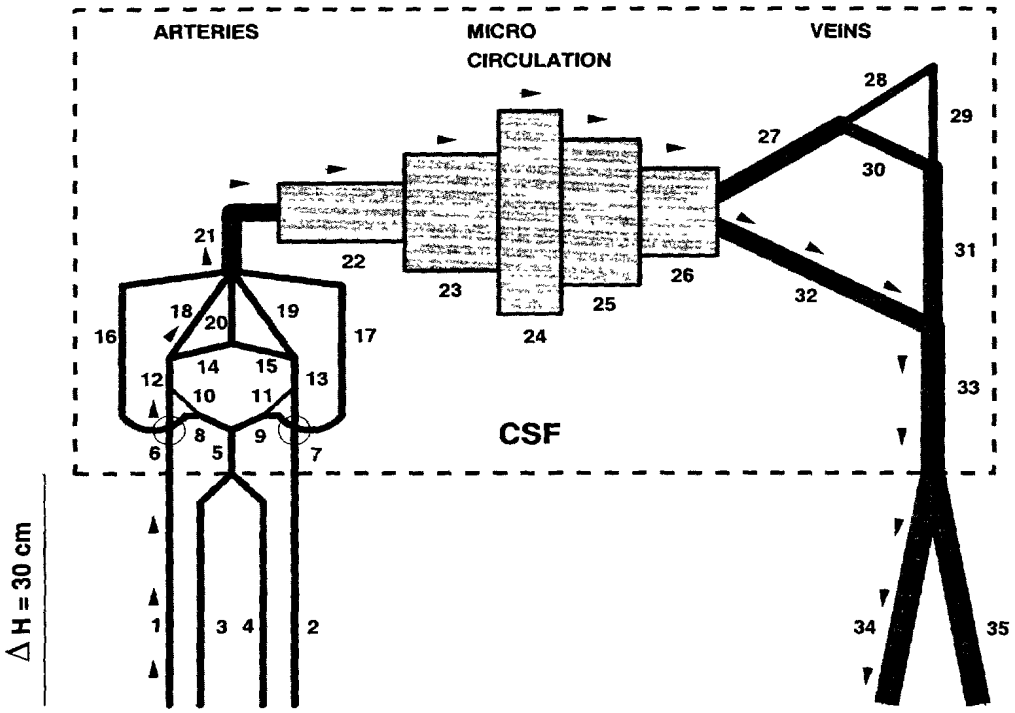

Fig. 1. Model of the cerebral circulation. The model begins at the root of common carotid and vertebral arteries, and ends with the internal jugular veins. The vessels surrounded by the broken line are intracranial vessels subjected to P_{CSF}. Arrows indicate the path used to illustrate the blood pressure drop for different values of G_z (Fig 2)

equal and opposite change of the CSF volume. Since the volume exchange between blood and CSF compartments occurs at the rate of approximately 0.5 $cm^3 \cdot min^{-1}$ (21), the cranial blood volume will remain constant at least over a period of several cardiac cycles. Therefore, P_{CSF} and the cranial blood pressure must be coupled in a way that preserves the net cranial blood volume, even when the blood pressure is significantly altered by gravitational effects. In other words, P_{CSF} is a function of G_z.

The aim of this paper is to examine the influence of the gravitational stress on cerebral vascular resistance and to assess the extent to which an increased vascular resistance plays a role in decreasing cerebral perfusion during G_z stress. The emphasis is on locating the most significant site of the G_z-induced resistance. The issue of the potential protective mechanism offered by the blood-CSF coupling is also addressed. We are focusing on the passive response of the cerebral vascular system subjected to a constant perfusion pressure and exposed to G_z stress. The active auto-regulation, i.e., change of blood vessel caliber induced by reflex mechanisms, is not incorporated in the model. The mathematical model of cerebral circulation is based on one-dimensional steady state equations of fluid dynamics, a non-linear relation between the transmural pressure and vessel area, and the assumption that the cranial blood volume is conserved.

METHODS

Model

The vessel network representing the cerebral circulation is shown in **Fig. 1.** The model geometry and morphological data are taken from Zagzoule and Marc-Vergnes (22), Sheng et al. (19), and Hillen et al. (10,9). The extracranial portion of the network is represented by carotid and vertebral arteries and by jugular veins, which are all assumed to extend vertically, from the heart level to the cranium. The intracranial vessels are oriented horizontally and are all assumed to be at the elevation of 30 cm above the heart. Smaller intracranial vessels are combined in parallel, and represented by equivalent vessels. The external pressure acting on the blood vessels inside of the cranium is that of the CSF. All the vessels are approximated to be axially uniform elastic tubes. Larger vessels are subdivided into smaller segments to allow spatial non-uniformity. Data used in the model are summarized in **Table I.**

Mathematical Formulation and Solution Procedure

Here we give a brief summary of the mathematical procedure used in the solution process. For a more thorough mathematical description of the problem, a precise definition of parameters, and a detailed explanation of the solution process, the reader should refer to the **Appendix.**

We examined steady blood flow in a branching network of elastic vessels partially subjected to a G_z-dependent external pressure. For each vessel segment, the balance of pressure and viscous forces is given by:

$$(P_1 + \rho G_z H_1) - (P_2 + \rho G_z H_2) = \mathcal{R}(A)\,LQ \qquad \text{Eq. 1}$$

where P_1, P_2 and H_1, H_2 are blood pressures and elevation at opposite vessel ends, respectively. L is the vessel length, Q is the flow-rate, and ρ is blood density. $\mathcal{R}(A)$ is the area-dependent laminar friction term (see

TABLE I. DATA USED IN THE MODEL.

Vessel No	Vessel	A_0 (cm^2)	L (cm)	EI (10^4 Pa)	h/r	n
1 & 2	Carotid arteries (extracranial)	0.14	30.0	13.67	0.25	1
3 & 4	Vertebral arteries	0.09	30.0	13.67	0.25	1
5	Basilar artery	0.14	3.0	27.35	0.25	1
6 & 7	Carotid arteries I (intracranial)	0.14	5.0	27 35	0.25	1
8 & 9	Posterior cerebral arteries I	0.07	2.0	27 35	0 25	1
10 & 11	Posterior communicating arteries	0.02	2.0	27.35	0.25	1
12 & 13	Carotid arteries II (intracranial)	0.14	2 0	27.35	0.25	1
14 & 15	Anterior cerebral arteries I	0.07	2.0	27.35	0.25	1
16 & 17	Posterior cerebral arteries II	0.07	7.0	30.08	0.25	1
18 & 19	Middle cerebral arteries	0.12	7.0	30.08	0 25	1
20	Anterior cerebral arteries II	0.12	7.0	30.08	0 25	2
21	Main branches of cerebral arteries	0.55	10 0	33.09	0.25	50
22	Pial network	1 75	2.0	36 40	0 25	3900
23	Intracerebral arteries	4.74	2.0	40.04	0.25	35000
24	Microcirculation	38.0	0.5	44.04		202000
25	Intracerebral veins	9.49	2.0	27.35	0.1	7200
26	Pial veins	3.86	2.0	13.0	0.1	3800
27	Cerebral veins I	0.92	5.0	5.17	0.1	40
28	Cerebral veins II	0.33	5.0	5.0	0.1	10
29	Longitudinal sinuses I	0.15	15.0	117.0		2
30	Veins	0.49	15.0	5.0	0.1	10
31	Longitudinal sinuses II	0.47	20.0	117.25		2
32	Veins	0.29	10.0	5.0	0.1	30
33	Transverse sinuses	1.65	5 0	117.78		1
34 & 35	Jugular veins	0.43	30.0	2.65	0 1	1

Appendix). The pressure-area relation for an elastic vessel is given by:

$$P - Pe = Kp\mathcal{F}(A/A_0) \qquad \text{Eq. 2}$$

where $P = (P_1 + P_2)/2$, Pe is the external pressure, A and A_0 are the cross-sectional area, and cross-sectional area at zero transmural pressure, respectively, while Kp is a constant describing the vessel wall elastic properties and thickness. The function $\mathcal{F}(A/A_0)$ for thin and thick-walled vessels is given in the Appendix. Conservation of the cranial blood volume is formulated as follows:

$$\sum_{i=1}^{k} (A(P, Pe) - A_0)_i L_i = 0 \qquad \text{Eq. 3}$$

where k is the total number of intracranial vessel segments. Applying the condition of mass and momentum conservation at the vessel junctions yields N non-linear algebraic equations, where N is the number of junctions in the network. The unknowns are blood pressures in the junctions and P_{CSF}. The (N + 1)-th equation is obtained from the conservation of the cranial blood volume.

The solution is obtained iteratively, each iteration containing three steps:

1. Blood pressures for each vessel segment are determined assuming that the vessels are rigid and with the cross-sectional areas determined in the previous iteration.
2. P_{CSF} is determined from the conservation of cranial blood volume (Eq. 3), using blood pressure from the current iteration.
3. New values of cross-sectional area are computed using Eq. 2 and the current values of the transmural pressure.

The process is repeated until the difference between the variables computed in two successive iterations is small enough.

RESULTS

Blood and CSF Pressure

Fig. 2 shows the pressure drop along the vascular tree, for three different values of G_z. The particular path chosen to be displayed is indicated by arrows in Fig. 1. For 0 G_z (i.e., the subject is lying in supine position) blood pressure remains positive everywhere in the system. Pressure changes are only due to viscous losses which, almost entirely, occur in the small cerebral arteries and micro circulation. For −5 G_z blood pressure

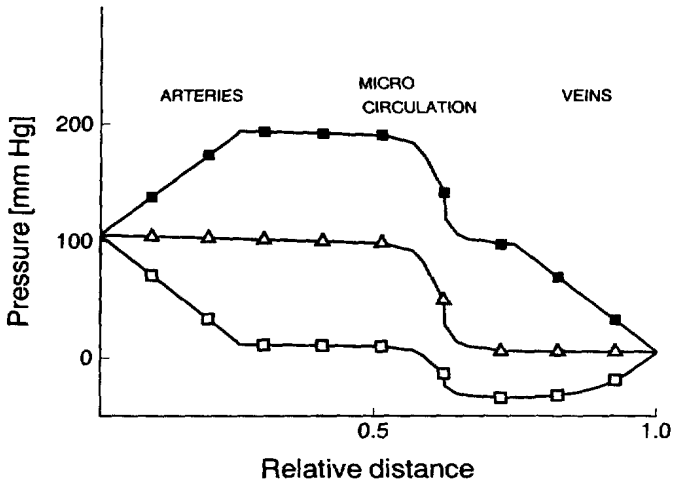

Fig. 2. Blood pressure drop along the vascular tree. △ = 0 G_z. ■ = −5 G_z. □ = +5 G_z The particular path chosen to be displayed is indicated by the arrows in Fig. 1.

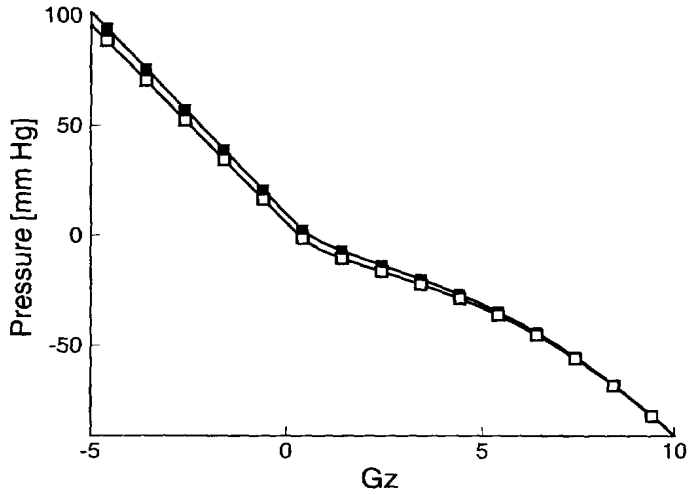

Fig. 3. CSF and the venous blood pressures for G_z ranging from −5 to +10 ■ = P_{CSF}. □ = Blood pressure in the cranial veins at the point where they join the dural sinuses. Note that P_{CSF} and the venous blood pressure always stay close regardless of G_z.

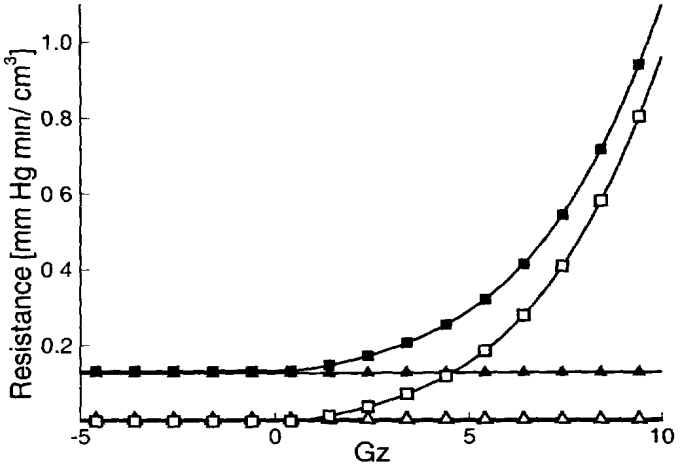

Fig. 4. Vascular resistance for G_z ranging from −5 to +10 ■ = total vascular resistance □ = vascular resistance of the jugular veins ▲ = vascular resistance of the cranial vessels. △ = vascular resistance of the extracranial arteries. Note that only the jugular resistance shows a strong dependence on G_z.

in the jugular veins is a linear function of the elevation, meaning that the hydrostatic effects dominate over the viscous effects. This indicates that the jugular veins are opened and that the siphon operates. The blood pressure is elevated in the intracranial vessels. However, the viscous drop in the intracranial vessels is of the same magnitude as in the case of 0 G_z. For +5 G_z blood pressure is negative at the level of cerebral micro circulation. The pressure curve on the venous side is no longer a straight line, indicating that the extracranial veins are collapsed and that their viscous resistance is significant. A much smaller pressure drop in the intracranial vessels is due to a decreased blood flow.

The relation between the G_z force and P_{CSF} is displayed by the line with solid squares in **Fig. 3.** The line with hollow squares shows the blood pressure in the intracranial veins at the point where they join dural sinuses. For 0 G_z the model predicts a P_{CSF} of 9 mm Hg which is well within the physiological limits (20). In the region where G_z is negative, P_{CSF} is essentially increased by the hydrostatic pressure of the blood column going from the heart to the head. Consequently, for −5 G_z P_{CSF} is approximately 100 mm Hg. In the positive G_z region P_{CSF} takes negative values before G_z reaches +1 and continues declining as G_z raises. The rate of decline is, however, much less steep than in the case when G_z is negative, and the nature of the relation is non-linear. The most interesting result is the fact that the venous and the CSF pressures stay close together for the whole range of G_z examined. Since the venous pressure is the lowest blood pressure in the cranium, the intracranial vessels should never be collapsed.

Vascular Resistance and Blood Flow

We examined the vascular resistance of three broad groups of vessels. The first group includes all extracranial arteries. The second involves all of the cranial vessels. The third group is the extracranial veins which in this model are represented by internal jugular veins. Vascular resistance is defined as:

$$R = \frac{\Delta(P + \rho G_z H)}{Q} \qquad \text{Eq. 4}$$

where $\Delta(P + \rho G_z H)$ is the blood and hydrostatic pressure difference driving the blood flow in a group of vessels (**Fig. 4**). The relation between the blood flow and G_z is shown in **Fig. 5.**

Several conclusions from the model results:

i) For zero and $-G_z$, total resistance is dominated by viscous losses in the small intracranial vessels. For $+G_z$, collapse of the extracranial vessels comes into play and the resistance rises exponentially with G_z. Consequently, at +4 G_z the cerebral blood flow is only 435 $cm^3 \cdot min^{-1}$, which is below the minimum required for maintaining normal brain function (14).

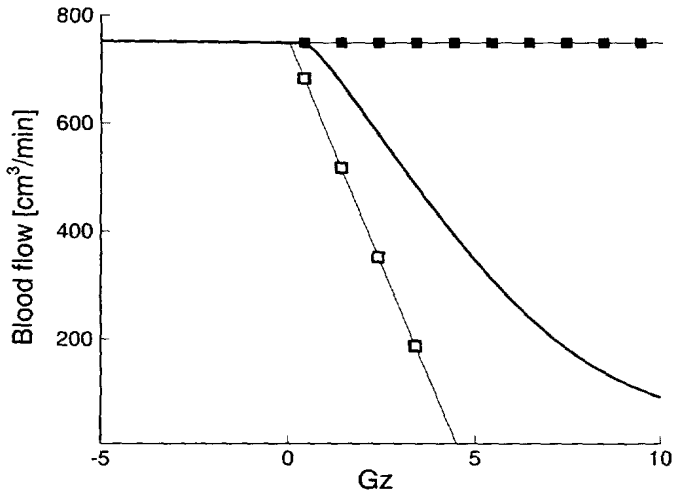

Fig. 5. Cerebral blood for G_z ranging from −5 to +10. Thick line: prediction of the model Thin line with solid squares. the case when the blood pressure in the veins experiences full recovery (rigid vessels) Thin line with hollow squares. the case in which the viscous pressure losses in the jugular veins exactly equal the hydrostatic pressure recovery.

ii) The intracranial vessels are subjected only to minor fluctuations of the transmural pressure when exposed to G_z and are protected from collapse. Consequently, the vascular resistance of the intracranial vessels is not dependent on G_z.

iii) The vascular resistance of the extracranial arteries is small and weakly dependent on G_z. The arterial resistance never contributes more than 3% to the total cerebral vascular resistance. The thick arterial walls make the collapse unlikely. For +10 G_z the increase in the arterial resistance is no more than 25% compared to the value at zero G_z.

iv) The jugular veins are the main contributor to the increase of the vascular resistance during positive G_z. Thin-walled veins are highly susceptible to collapse. When G_z is positive, the blood pressure experiences its lowest value at the point where dural sinuses drain into jugular veins. Of all the sites in the system, this is the one where the collapse is most likely to occur. Before G_z reaches the value of +5, the venous resistance will equal the cranial resistance thus effectively doubling the total resistance and cutting blood flow in half.

DISCUSSION

Vascular Resistance

This study indicates that even if the normal perfusion pressure is maintained, the increase in the vascular resistance caused by the gravitational stress may lead to inadequate cerebral perfusion. There is a substantial difference in the extent to which different portions of the vascular system respond to G_z stress. Three broad groups of vessels can be distinguished in that sense. The first group are the large thick-walled extracranial arteries, which do not collapse and have very low resistance to flow for all values of G_z examined. The second group are the cranial vessels. Although this group is morphologically very diverse, protection from the collapse provided by the CSF is common for all vessels. This group is characterized by a substantial resistance which is, however, independent of G_z. The third, and in a sense the most interesting group, are the extracranial veins characterized by thin compliant walls and with resistance extremely dependent on G_z. In fact, this is the only group significantly affected by the gravitational effects. We will use a simple mathematical example to illustrate the significance of the venous portion of the vascular system. Denote the left ventricular pressure by P_{VEN}. We assume no resistive losses in the extracranial arteries, but there is a hydrostatic pressure drop of $\rho G_z \Delta H$, where ΔH is the height of the blood column from the heart to the head. Flow through the constant cranial resistance R_C causes a further pressure drop QR_C. Finally, in the extracranial veins the blood experiences a hydrostatic pressure rise of $\rho G_z \Delta H$ and a resistive drop of $QR_V(G_z)$, where $R_V(G_z)$ is the jugular resistance. Thus, the atrial pressure P_{ATR} is given by,

$$P_{ATR} = P_{VEN} - \rho G_z \Delta H - QR_C + \rho G_z \Delta H - QR_V(G_z) \quad \text{Eq. 5}$$

Note that the hydrostatic terms cancel and the equation can be rearranged to give

$$Q = \frac{\Delta P}{R_C + R_V(G_z)} \quad \text{Eq. 6}$$

where ΔP is the perfusion pressure ($P_{VEN} - P_{ATR}$). Obviously, R_V is the only G_z-dependent parameter which affects the blood flow, providing that ΔP is constant. It is important to note that R_V is in fact the function of the transmural pressure only and that it can take different values for the same G_z if blood pressure or external pressure are altered for the reasons other than the gravitational stress.

The effect of the G_z-dependent jugular resistance can be discussed in terms of the extent to which pressure recovers as the blood descends towards the heart. If the veins were rigid, R_V would have been constant and negligible, the blood pressure at the point where the jugular veins leave the skull would be $P_{ATR} - \rho G_z \Delta H$, and the blood flow would be:

$$Q_{MAX} = \frac{\Delta P}{R_C} = \text{const.} \quad \text{Eq. 7}$$

(faint line with solid squares in Fig. 5). The other extreme case is the one in which viscous losses in the jugular veins exactly equal the hydrostatic pressure component ($R_V Q = \rho G_z \Delta H$). In this case blood pressure is P_{ATR} everywhere in jugular veins, and blood flow is given by:

$$Q_{MIN} = \frac{\Delta P - \rho G_z \Delta H}{R_C} \quad \text{Eq 8}$$

(faint line with hollow squares in Figure 5). In other words, blood flow is possible only if the perfusion pressure is higher then the hydrostatic pressure of the blood column going from the heart to the head, meaning that it would be zero at approximately +4.5 G_z. This case was discussed by Pedley et al. (15) in the study of blood flow in giraffe jugular vein. The blood flow predicted by our model is somewhere in between these two extreme cases (thick line in Fig. 5). According to the model, the jugular blood pressure at the head level approximately equals P_{CSF}. Therefore, the blood flow predicted by the model is roughly:

$$Q = \frac{(P_{VEN} - \rho G_z \Delta H) - P_{CSF}}{R_C} \quad \text{Eq. 9}$$

Since P_{CSF} is negative for $+G_z$, $Q > Q_{MIN}$ indicating that the gravitational pressure recovery exists even when the veins are considerably narrowed. This is in agreement with experimental results performed on a mechanical model by Hicks and Badeer (8). They measured pressure in an inverted U tube with a flexible descending limb and found that the gravitational pressure recovery is present in the partially collapsed descending tube. Henry et al. (7) report that the negative blood pressure in the jugular veins facilitates blood flow in a subject exposed to acceleration stress.

CSF Pressure

Rushmer et al. (18) measured blood and CSF pressure in cats exposed to positive and negative G_z and con-

cluded that P_{CSF} and venous pressure always stay roughly the same. Our model leads to the same conclusions using the assumption that the cranial blood volume is conserved. Since blood pressure decreases along the cranial vascular tree, total blood volume can be conserved only if some vessels are distended while others are collapsed. It is reasonable to assume that the collapse occurs after the level of micro circulation where blood pressure experiences a substantial drop. Therefore, P_{CSF} must be lower than the arterial but higher than the venous pressure. A more precise assessment of P_{CSF} in relation to arterial and venous pressures can be obtained by considering elastic properties of the cranial blood vessels and the pressure-area relation for collapsible tubes. Arteries have thick and stiff walls. In addition they are distended, meaning that their compliance is very low (see the Appendix for the tube law). Therefore, the cranial arterial blood volume will not be very sensitive to changes in the transmural pressure. On the other hand veins are thin walled, much less stiff than arteries, and at least some of them are partially collapsed. They are, therefore, extremely compliant and sensitive to changes in the transmural pressure. Cranial blood volume is conserved if the increase of the arterial blood volume is matched by an equivalent decrease of the venous blood volume. It is clear from the above discussion that if P_{CSF} is to produce exactly the same volume change on the arterial and venous side, it should be much closer to venous than to arterial blood pressure. Indeed, the model predicts that the conservation of blood volume requires that P_{CSF} be only several millimeters of mercury higher than the lowest venous pressure in the system.

Anti-G Suits and Positive Pressure Breathing

The indications that the patency of the jugular vein is the critical physiological factor in GLOC, may affect how anti-G_z garmentry, straining maneuvers, and PPB are utilized in providing optimal G_z protection, especially during push-pull maneuvers (1). Too early application of any anti-G technique may have deleterious effects on both the venous and arterial sides. Any elevation of arterial pressure prior to the onset of G_z would result in baroreceptor activation. This may lead to a decrease in heart rate, a decrease in stroke volume, and peripheral vasodilation just as the G_z onset occurs, and no real increase in perfusion pressure. Elevation of both arterial and venous pressure with the onset of G_z, such as to maximize perfusion pressure, stimulate baroreceptor reflexes, and minimize cerebrovascular resistance would be desired. Due to developments in advanced anti-G_z protection systems and the recognition of the importance of the G_z-time history in determining the instantaneous G_z tolerance of the pilot (1), a better understanding of the mechanisms involved in G_z susceptibility and G_z tolerance, and how and why anti-G_z techniques work (including straining maneuvers, postural adjustments, anti-G suits, and PPB), could be incorporated into the design of control algorithms for computer controlled anti-G valves and breathing regulators.

Limitations

By examining only the mechanical side of the cerebrovascular system, some potentially important mechanisms such as cerebral autoregulation are ignored. It is well known that caliber of the intracranial vessels change in response to changes in carbon dioxide and oxygen and that cerebral blood flow remains fairly constant when the arterial pressure is between 60 and 140 mm Hg (5). This mechanism may be important, at least at moderate $+G_z$. The results for $-G_z$ simply indicate that there is no purely mechanical mechanism which would cause impairment of the cerebrovascular system under $-G_z$. In reality, however, the action of cardiovascular reflexes and the physical discomfort will severely limit the performance of the pilot (11).

As far as the CSF dynamics is concerned, we did not take into account the process of CSF production and absorption which can cause interchange between the CSF and blood volume in the skull. Apart from the argument that this process is normally too slow to be important for the time scale of interest, the model shows that transmural pressures at the level of the choroid capillary and sagittal sinus, which are believed to govern CSF production and absorption (21), are independent of G_z.

The fact that the flow is assumed to be steady, and that physiological reflexes are not incorporated implies that the model is valid only for sustained G_z. It has been shown that for the rapid G_z onset the arterial pressure at the head level is time dependent rather than simply a function of the hydrostatic gradient (4). Reflex response is even more important in the case of complex G_z profiles such as push-pull (1), where transient behavior of the system is essential.

Finally, since the model is open-loop, the influence of the rest of the cardiovascular system, including the heart, can be accounted for only by manipulating the boundary conditions. We have deliberately chosen to fix the pressures at the level of the heart in order to examine whether the flow rate will be altered by G_z even if the central blood pressures are maintained at their normal values. When the protective measures such as straining, G-suit, or PPB are concerned, their impact can be discussed only in terms of the changes they cause in the pressures at the model ends. An increased blood flow can be a result of increased perfusion pressure, decreased vascular resistance, or both. However, since one of the goals of the protective measure and the cardiovascular reflexes is to maintain normal cardiac output, the current results can be regarded as a best case analysis of the mechanical effects of G_z on cerebral perfusion.

CONCLUSIONS

For the parameter values considered, the cross-sectional areas and resistances of both the extracranial arteries and the intracranial vessels are very insensitive to the purely mechanical effects of G_z. For sustained G_z, assuming that normal central blood pressures are maintained by effective cardiovascular reflexes and life support intervention, cerebral blood flow is reduced. This is

primarily a result of the increased resistance of the veins outside of the skull. For G_z greater than approximately 4.5, the arterial blood pressure at the head is negative. Blood flow is maintained by a siphon effect. However, because of the increased jugular resistance, the flow rate is below the level needed to support normal brain function.

The cerebrospinal fluid pressure is determined by the fact that the cranial volume is fixed. The central venous pressure and the venous vascular resistance are important parameters in this mechanism.

Despite the limitations discussed above, this model provides an interesting insight into the mechanical factors governing cerebral perfusion. In particular, it reveals the controlling influence of the collapsed jugular vein. Our long term goal is to predict physiological response to complex G_z histories. This will require a closed loop model incorporating cardiovascular reflexes and life support systems.

APPENDIX

The Governing Equations

The equations governing one-dimensional flow in vessels with compliant walls are as follows (3,22,19):

Fluid continuity

$$\frac{\partial A}{\partial t} - \frac{\partial Q}{\partial x} = 0 \qquad \text{Eq. 10}$$

where x is the spatial coordinate aligned with the vessel axis.

Fluid momentum

$$\rho\left(\frac{\partial U}{\partial t} + U\frac{\partial U}{\partial x}\right) = -\frac{\partial P}{\partial x} - \mathcal{R}(A)Q + \rho G_z \cos\alpha \qquad \text{Eq. 11}$$

U is the fluid velocity, α is the angle between x and the direction of the gravitational force, and the friction factor $\mathcal{R}(A)$ is given following Cancelly and Pedley (3):

$$\mathcal{R}(A) = \begin{cases} 8\pi n\mu/A^2 & \text{if } P - Pe > Pc \\ 8\pi n\mu A_0/A^3 & \text{otherwise} \end{cases} \qquad \text{Eq. 12}$$

where Pc is the critical transmural pressure at which the vessel loses stability and collapses, μ is the dynamic coefficient of viscosity for blood, and n is the number of vessels in parallel, in case of the equivalent vessels

Tube law

$$P - Pe = Kp\mathcal{F}(A/A_0) \qquad \text{Eq. 13}$$

The constant Kp is defined as·

$$Kp = \begin{cases} El = Eh/2r & \text{if } P - Pe > Pc \\ Eh^3/12r^3\sqrt{(1-\sigma^2)} & \text{otherwise} \end{cases} \qquad \text{Eq. 14}$$

Where E and σ = 0.5 are the Young's modulus and the Poisson's coefficient of the vessel wall material, respectively, h is the wall thickness, r is the radius of the vessel, and El is the elastance. For thin walled vessels (veins) Pc = 0, for thick walled vessels (all other vessels) we use:

$$Pc = -\frac{Eh^3}{4r^3\sqrt{(1-\sigma^2)}} \qquad \text{Eq 15}$$

The function $\mathcal{F}(A/A_0)$ is given by:

$$\mathcal{F}(A/A_0) = \begin{cases} (A/A_0) - 1 & \text{if } P - Pe > Pc \\ Pc/Kp + \alpha_c^{-3/2} - (A/A_0)^{-3/2} & \text{otherwise} \end{cases} \qquad \text{Eq. 16}$$

Where α_c is the relative area at the point where a vessel starts collapsing·

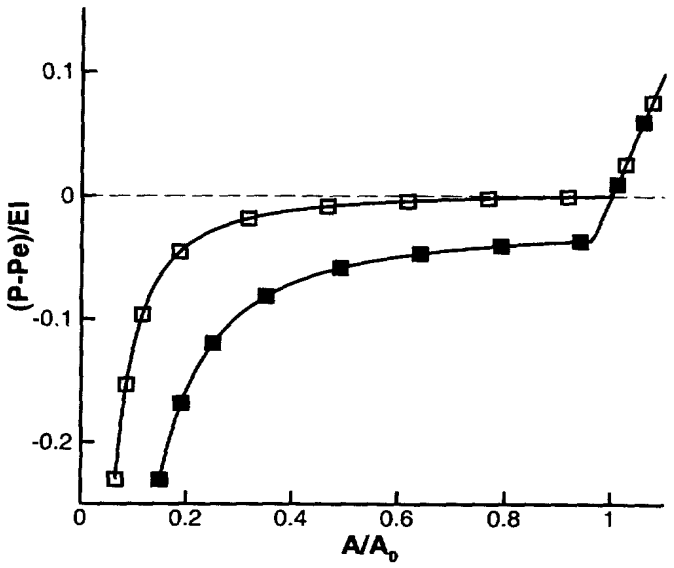

Fig. 6. Pressure-area relation for thick-walled and thin-walled elastic vessels. The area is normalized with respect to the area at zero transmural pressure. The transmural pressure is normalized with respect to the elastance. ■ = thick-walled vessel (h/r = 0.25). □ = thin-walled vessel (h/r = 0.1).

$$\alpha_c = 1 + \frac{2rPc}{Eh} \qquad \text{Eq. 17}$$

The function $\mathcal{F}(A/A_0)$ (**Fig. 6**) is essentially the one used by Bertram and Pedley (2) with a modification introduced to account for the fact that the thick-walled vessels do not collapse immediately after the transmural pressure becomes negative.

Steady Flow in a Single Vessel

When the flow is steady, equations 10 and 11 reduce to:

$$Q = \text{const.} \qquad \text{Eq. 18}$$

and

$$\frac{\partial}{\partial x}\left(\rho\frac{U^2}{2} + P + \rho G_z H\right) = \mathcal{R}(A)Q \qquad \text{Eq. 19}$$

Now we introduce the assumption that the vessel area is spatially uniform This means that both the original vessel area as well as changes in vessel area are constant spatially. This is a valid assumption when pressure variations in a vessel are small. When the vessel is long enough that significant pressure variations can be expected due to viscous or gravitational effects, it is subdivided into smaller segments. Eq. 19 can be integrated with respect to x and combined with Eq. 18 to yield Eq. 1.

Steady Flow in a Branching Network of Vessels

At each vessel junction the conservation of mass and momentum is given by:

$$\sum_{i=1}^{i=k} Q_i = 0 \qquad \text{Eq. 20}$$

and

$$(P + \rho U^2/2)_i = (P + \rho U^2/2)_j; \quad i = 1, \ldots k; \quad j = 1, \ldots k \qquad \text{Eq. 21}$$

where k is the number of vessels in the junction. Assuming that $\rho U^1/2$ is small compared to P, Eq. 21 reduces to.

$$P_i = P_j; \quad i = 1, \ldots k; \quad j = 1, \ldots k \qquad \text{Eq. 22}$$

In words, in order that mass and momentum be conserved at a tube junction, the sum of all the blood entering and leaving the junction

must be zero, and the blood pressure at the point of junction must be the same for all the vessels in the junction Using Eq. 20 and Eq. 21, the conservation of mass at a junction can be expressed as.

$$\sum_{i=1}^{k}\left[\frac{(P_1+\rho G_z H_1)-(P_2+\rho G_z H_2)}{\mathcal{R}(A)L}\right]_i=0 \qquad \text{Eq 23}$$

Applying the conservation of mass to every junction in the network, and using the tube-law and the conservation of cranial blood volume leads to a system of algebraic equations, the solution of which yields blood pressures, vessel areas and P_{CSF} in the network. Since the system is non-linear, an iterative procedure is used.

1 When the vessels are assumed to be rigid, the area is independent of the transmural pressure In this case, applying the conservation of mass to all the junctions will lead to a system of linear algebraic equations which can easily be solved to yield the blood pressure at the junctions. Therefore, in each iteration we assume that the vessels are rigid and have a cross-sectional area from the previous iteration Thus, solving the system of linear algebraic equations we obtain the blood pressure at the junctions for the current iteration
2. In the next step we determine P_{CSF} for the current iteration using the conservation of the cranial blood volume. For vessels with spatially uniform cross-sectional area, the conservation of the cranial blood volume takes the form expressed in Eq. 3. Combining Eq. 3 and the tube law we have

$$\sum_{i=1}^{m}\left\{A_0 L\left[\mathcal{F}\mathcal{J}\left(\frac{P-P_{CSF}}{Kp}\right)\right]\right\}_i=0 \qquad \text{Eq. 24}$$

where m is the number of cranial vessels and $\mathcal{F}\mathcal{J}$ is the inverse of $\mathcal{F}$

$$\mathcal{F}\mathcal{J}\left(\frac{P-P_{CSF}}{Kp}\right)=\begin{cases}[(P-P_{CSF})/Kp+1] \text{ if } P-Pe>Pc\\ [\alpha_c^{-3/2}-(P-P_{CSF}-Pc)/Kp]^{-2/3} \text{ otherwise}\end{cases} \qquad \text{Eq. 25}$$

Eq 24 is a single non-linear algebraic equations in terms of P_{CSF} which can be solved using Newton-Raphson method (16).
3. Knowing P and P_e we can calculate vessel area using the tube law.

These three steps give P, P_{CSF} and A for a single iteration The process is repeated until the difference between the variables computed in two successive iterations is small enough.

ACKNOWLEDGMENTS

This work has been generously supported by the Canadian Department of National Defence.

REFERENCES

1. Banks RD, Grisset JD, Saunders PL, et al. The effect of varying time at −Gz on subsequent +Gz physiological tolerance (push-pull effect). Aviat Space Environ Med 1995; 66.723–7
2. Bertram CD, Pedley TJ. A mathematical model of unsteady collapsible tube behaviour. J Biomech 1982; 15 39–50
3. Cancelli C, Pedley TJ A separated-flow model for collapsible tube oscillations. J Fluid Mech 1985, 157:375–404.
4 Gillingham KK, Freeman JJ, McNee RC Transfer functions for eye-level blood pressure during +Gz stress Aviat Space Environ Med 1977, 48 1026–34
5 Guyton AC, Hall JE. Textbook of medical physiology. Philadelphia: W B. Saunders Company, 1996.
6. Hamilton WF, Woodbury RA, Harper HT. Arterial cerebrospinal and venous pressures in man during cough and strain. Am J Physiol 1943; 141 42–50.
7. Henry PJ, Gauer OH, Kety SS, Kramer K. Factors maintaining cerebral circulation during gravitational stress. J Clin Invest 1951; 30·292–300.
8 Hicks JW, Badeer HS Siphon mechanism in collapsible tubes: application to circulation of the giraffe head. Am J Physiol 1989; 256:R567–R571.
9 Hillen B, Drinkenburg BAH, Hoogstraten HW, Post L Analysis of flow and vascular resistance in a model the circle of willis. J Biomech 1986, 21:807–14.
10. Hillen B, Hoogstraten HW, Post L. A mathematical model of the flow in the circle of willis J Biomech 1984; 19:187–94.
11 Howard P. The physiology of negative acceleration. In: Gillies JA, ed. A textbook of aviation physiology. New York: Pergamon Press, 1965 688–716.
12. Howard P The physiology of positive acceleration. In· Gillies JA, ed. A textbook of aviation physiology New York: Pergamon Press, 1965 551–687.
13. Kety SS, Henry AS, Shmidt CF. The effect of increased intracranial pressure on cerebral circulatory function in man. J Clin Invest 1947; 27:493–9
14 Kety SS, Henry AS, Shmidt CF. The effect of increased intracranial pressure on cerebral circulatory function in man. J Clin Invest 1947; 27·493–9.
15 Pedley TJ, Brooks BS, Seymour RS Blood pressure and flow rate in the giraffe jugular vein. Phil Trans R Soc Lond 1996; 352: 855–66.
16 Press WH, Teukolsky SA, Vetterling WT, Flannery BP. Numerical recipies in Fortran· the art of scientific computation. New York· Cambridge University Press, 1986.
17. Ruan JS, Khalil T, King AI. Human head dynamic response to side impact by finite element modeling. J Biomech Eng 1991, 113 276–82.
18. Rushmer RF, Beckman EL, Lee D Protection of the cerebral circulation by the cerebrospinal fluid under the influence of radial acceleration. Am J Physiol 1947, 151:459–68.
19. Sheng C, Sarwal SN, Watts KC, Marble AE. Computational simulation of blood flow in human systemic circulation incorporating an external force field. Med Biol Eng Comput 1995, 33:8–17.
20. Takemae T, Kosugi Y, Ikebe J, et al. A simulation study of intracranial pressure increment using an electric circuit model of cerebral circulation IEEE Trans Biom Eng 1987; 34.958–62
21 Ursino M. A mathematical study of human intracranial hydrodynamics part 1—the cerebrospinal fluid pulse pressure Ann Biomed Eng 1988; 16:379–401
22. Zagzoule M, Marc-Vergnes JP. A global mathematical model of the cerebral circulation in man. J Biomechanics 1986, 19:1015–22.

#513877